Fish and Shellfish Immunology 84 (2019) 937–947

Contents lists available at ScienceDirect

Fish and Shellfish Immunology

journal homepage: www.elsevier.com/locate/fsi

Full length article

Transcriptome analysis of immune response in fat greenling (*Hexagrammos otakii*) against *Vibrio harveyi* infection

Jing Diao, Hongjun Liu, Fawen Hu, Le Li, Xiaolu Wang, Chunlei Gai, Xiaoqing Yu, Ying Fan, La Xu, Haibin Ye*

Shandong Key Laboratory of Disease Control in Mariculture, Shandong Mariculture Institute, No 7, Youyun Road, Qingdao, 266104, PR China

ARTICLE INFO

Keywords:
Transcriptome
Fat greenling (*Hexagrammos otakii*)
Vibrio harveyi
Immune response

ABSTRACT

Fat greenling (*Hexagrammos otakii*) is an important aquaculture fish species in northern China. Unfortunately, *Vibrio* infections have caused considerable losses to the fat greenling aquaculture industry. However, the study on immune response of fat greenling against *Vibrio* species has not been reported yet. In this paper, the immune response of fat greenling against *V. harveyi* at gene expression level was studied by transcriptome analysis. A total of 189753 high-quality unigenes with a N50 length of 672bp were obtained by transcriptome profiling, which provided abundant data for the future study of fat greenling. Comparative analysis showed that 5425 differentially expressed genes (DEGs) were identified on day 3 post-infection (3dpi), containing 1837 up-regulated and 3588 down-regulated genes. Further annotation and analysis revealed that the DEGs were enriched in complement and coagulation cascades, ribosome, oxidative phosphorylation, glycine, serine and threonine metabolism and peroxisome proliferator-activated receptor (PPAR) signaling pathway. These pathways were mainly associated with phagocytosis and pathogen clearance, rarely involved in bacteria adhesion and pathogen identification, which suggested that the host might begin to clear and kill the invading bacteria on 3dpi. The research might provide a valuable resource to further study immune response and suggest strategies against *V. harveyi* infection in fat greenling.

1. Introduction

Fat greenling (*Hexagrammos otakii*) is one of the most important commercial marine fish species owing to its high-quality meat. In China, fat greenlings are mainly distributed in the Yellow Sea, the Bohai Sea and the East China Sea [1,2]. Unfortunately, the frequent outbreaks of disease have become an important factor restricting the development of healthy aquaculture of fat greenling, especially bacterial disease [3]. Vibriosis is a severe and important disease reported from a large number of marine and freshwater fish species and causes great economic loss worldwide [4–6]. Recent years, the cultured fat greenling also suffered from Vibrio infections and caused the reduction in production in China. However, there is still lack of attention to the diseases and immunity of fat greenling.

Vibrio harveyi is a luminescent gram-negative bacterium and widely reported in the marine environment, which exists as a free-living as well as commensal pathogen in the enteric guts of marine animals [7]. This bacterium is a major pathogen that causes the outbreak of vibriosis in aquatic vertebrates and invertebrates, leading to massive deaths in course of the production [8]. To date, many teleosts infected by *V. harveyi* have been reported, such as Atlantic salmon (*Salmo salar*), common snook (*Centropomus undeeimalis*) and flounder (*Paralichthys olivaceus*) [9–11]. To prevent and control vibriosis caused by *V. harveyi*, many studies have been carried to explore its pathogenesis, and the studies on fish immune response against *V. harveyi* also have been reported in many teleosts [12–14]. However, there was no study on immune response of fat greenling against *V. harveyi* infection, which increase the difficulties of using immunological methods to prevent and control vibriosis caused by *V. harveyi* during the cultivation.

Transcriptome profiling using next-generation sequencing (NGS) technologies can study the transcription of genes and the regulation of transcriptional at the overall level. In common carp (*Cyprinus carpio*), transcriptome analysis shows that the expressions of many genes significantly up-regulated or down-regulated after *Aeromonas hydrophila* infection, and the differentially expressed genes (DEGs) are enriched in the pathways of junction/adhesion, pathogen recognition, cell surface receptor signaling, and immune system process/defense response [15]. It's also reported that the DEGs are mainly involved in immune-related

* Corresponding author.
E-mail address: yehaibin@263.net (H. Ye).

https://doi.org/10.1016/j.fsi.2018.10.067
Received 16 July 2018; Received in revised form 16 October 2018; Accepted 24 October 2018
Available online 25 October 2018

pathway functions, NOD-like receptor signaling pathways, Toll-like receptor signaling pathways, NF-κB signaling pathways, and Jak-STAT signaling pathways in orange-spotted grouper after *V. harveyi* infection [16]. Besides, the DEGs are also revealed against bacterial infections in other teleosts using transcriptome profiling, such as Antarctic notothenioid fish (*Notothenia coriiceps*), Asian seabass (*Lates calcarifer*), Nile tilapia (*Oreochromis niloticus*) [17–20]. Transcriptome profiling has provided new insights into immune responses against bacterial infections in various aquaculture animals. However, many studies using transcriptome profiling have focused on immune response of host within 48 h after bacterial infection, few reports are performed to investigate the immune response of host on day 3 post-infection (3dpi), which might provide more information on the immune response of fish against bacterial infection.

In this study, we analyzed immune response of fat greenling on 3dpi of *V. harveyi* using transcriptome profiling. The transcriptome profiles will provide more information on the fat greenling gene sequence, and the information of DEGs following *V. harveyi* infection may provide a valuable resource for further research and suggest strategies for the prevention and control of *V. harveyi* infection.

2. Materials and methods

2.1. Bacteria challenge and sample collection

100 healthy fat greenling with body weights of 30 ± 5 g were obtained from a fish farm in Rizhao of Shandong province, China. The fish were maintained in tanks containing aerated sand-filtered seawater at 20 ± 0.5 °C for one week prior to processing. Then fat greenling was randomly divided into two groups. The strain of *V. harveyi* SD201506 was isolated from the spleen of diseased fat greenling and proved to be a pathogenic strain by infection experiment previously by our laboratory. The LD_{50} of *V. harveyi* was determined to be 5×10^6 CFU/fish to fat greenling with an average weight of 30 g. For challenge, the concentration of *V. harveyi* bacterial suspension was adjusted to 5×10^7 CFU/ml, and each fish was intraperitoneally injected with 100 μl bacterial suspension. In the control group, the fish was intraperitoneally injected with 100 μl PBS.

Three days after infection, 15 fish from each group were randomly selected and divided into 3 replicates (5 fish per replicate). After anaesthetizing with MS-222, the spleens were collected and immediately submerged into 10 ml RNAlater™ (Ambion, USA). Tissues were stored at −80 °C until RNA extraction.

2.2. RNA isolation and illumina sequencing

Samples were homogenized with sterilized mortar and pestle in the presence of liquid nitrogen to a fine powder. Total RNA was extracted from tissue using the RNeasy Plus Mini Kit (Qiagen, USA) following the manufacturer's instruction. RNA quality was verified using a Bioanalyzer 2100 (Agilent Technologies, Santa Clara, CA, USA). RNA from each mixed sample was divided into two parts: one for transcriptome sequencing and the remaining part for quantitative real-time PCR (qRT-PCR) to validate the reproducibility of DEGs data obtained from transcriptome sequencing.

The cDNA libraries for transcriptome sequencing were generated using TruSeq™ RNA Sample Preparation Kit (Illumina, USA) following the manufacturer's instruction. Briefly, total RNA was performed to isolate mRNA by poly-T oligo-attached magnetic beads. First-strand cDNA was synthesized using random hexamer primers and Superscript III Reverse Transcriptase (Invitrogen, USA). This step was followed by synthesis of second-strand cDNA, end repair, and ligation of adaptor. The size and total concentration of cDNA libraries were examined by Agilent 2100 Bioanalyzer and fluorescence quantitative, respectively. Then, the sequencing was carried out by Personal Biotechnology Company (Shanghai, China) using Illumina NextSeq500 platform.

2.3. Transcriptome assembly and annotation

The protocols of transcriptome assembly and annotation were provided by Personal Biotechnology Company (Shanghai, China). Briefly, the quality of raw data was firstly analyzed using FastQC software after running TopHat. Then, raw data were filtered by removing adaptors and low quality reads to obtain clean reads. The clean reads were spliced and assembled into transcript using Trinity software, and the longest transcript under each gene was extracted as unigene [21].

The unigenes function was annotated according to the five databases: Nr (NCBI non-redundant protein sequences), eggNOG (evolutionary genealogy of genes: Non-supervised Orthologous Groups), Swissprot (A manually annotated and reviewed protein sequence database), GO (Gene Ontology), and KO (KEGG Ortholog database) using BLAST with a cutoff *E*-value of 10^{-5}.

2.4. Quantification of gene expression levels and differential expression analysis

Gene expression levels of the samples were estimated using RSEM (RNA-Seq by Expectation Maximization, rsem-1.2.0), a user-friendly software package for quantifying gene abundances from paired-end RNA-seq data [22]. Clean data were matched with the assembled transcriptome. Readcount of each unigene was derived from the mapping results and then normalized to FPKM (expected number of Fragments Per Kilobase of transcript sequence per Millions base pairs sequenced) [23].

Differential expression analysis of spleen potentially involved in *V. harveyi* infection was analyzed using the package DEG-seq with biological replicates [24]. DEG-seq provided statistical method to determine differential expression genes; the false discovery rates were limited by adjusting the resultant *p*-values employing the reported methods [25]. Genes with an adjusted *p*-value ≤ 0.05 and fold change > 2 were set as the threshold for significantly differential expression.

2.5. GO/KEGG enrichment analysis for DEGs

For gene ontology analysis, the alignment results were parsed for assigning GO terms by using Blast2GO software. The DEGs of fat greenling spleen were aligned against Gene Ontology database. The study set represented the GO terms of all identified DEGs. The calculated *p*-value goes through Bonferroni Correction, taking corrected *p*-value ≤ 0.05 as a threshold.

According to the KEGG database resources, pathway enrichment analysis were carried to further seek out the notably enriched signal transduction pathways or metabolic pathways. The statistical enrichment of DEGs in KEGG pathways was detected using KOBAS software (v2.0) [26].

2.6. Quantitative real-time PCR validation

To validate the reliability of DEGs data obtained from the transcriptome sequencing in spleen of fat greenling, qRT-PCR was conducted on 12 randomly selected DEGs according to established protocols with some modifications [27]. Briefly, the same batch of RNA samples as sequenced was used, and the first-strand cDNA was synthesized using the SuperScript® III RT kit (Invitrogen, USA) according to the manufacturer's instructions and diluted to 100 ng/μl for qRT-PCR. The qRT-PCR was carried out using SYBR GreenIMaster (Roche, CH) in a LightCycler® 480 II Real Time System (Roche, CH). Each assay was performed in triplicate with elongation factor 1β gene as the internal reference. All dates were analyzed relative to the elongation factor 1β gene by the $2^{-\triangle\triangle Ct}$ method, then difference in the infection and control groups were employed to assess changes in the expression of genes. All primers were designed according to the corresponding sequences and listed in Table 1.

Table 1
Sequences of primers used in qRT-PCR analysis.

Primer name	Sequence (5′-3′)
qRT-PCR-KLF9-like-F:	TGAATAAATGCAACCCAAAC
qRT-PCR-KLF9-like-R:	CCGTACATCTTCCCACAGC
qRT-PCR-Stanniocalcin-2-like-F:	AACCTGTGCTCTGCTGCTA
qRT-PCR-Stanniocalcin-2-like-R:	CAATGCCTCCTTAACCTCC
qRT-PCR-Gremlin2-like-F:	TCAGACAATCAGCGAGGAG
qRT-PCR-Gremlin2-like-R:	AAGGAGCAGGACTGGAACG
qRT-PCR-Cdkn 1-F:	CGGTATGGATGTACTGGAGCG
qRT-PCR-Cdkn 1-R:	GAAGTCTGTGATGTGCGTGTTG
qRT-PCR-RGS-F:	ACTTGGAATCTATCCTGCTGC
qRT-PCR-RGS-R:	GCTTTGGCTGGTAATTTGGT
qRT-PCR-Glutamate receptor-F:	GAGTTCTGGCTCACTTCGC
qRT-PCR-Glutamate receptor-R:	TGGTCGCACGCTCTTCTTG
qRT-PCR-IL-12β-F:	CTCTGATTGGCTGCTGCTCC
qRT-PCR-IL-12β-R:	GACGGGTCCAGAGCCAGTAA
qRT-PCR-Integrin α-6-F:	TCTGTTTAGGGTGACCAAGGAA
qRT-PCR-Integrin α-6-R:	CTTGAGATAGGACGGGAGGG
qRT-PCR-Claudin 3-F:	CCTGTAGCGATGTGTCTCCC
qRT-PCR-Claudin 3-R:	TCCCTCAAAAGGACAACGCC
qRT-PCR-TfR 1-like-F:	GTCTCTGGCGAACAAGGTGA
qRT-PCR-TfR 1-like-R:	AGGTTGATGCTCTTGTCCCG
qRT-PCR-GIMAP-F:	AGTCGTTCTGGCGATGGTTAT
qRT-PCR-GIMAP-R:	TGTTGTCTGTCAGTGGGTTTT
qRT-PCR-Sart-F:	AGAGCAGAAGCAGCCAGAT
qRT-PCR-Sart-R:	GTCCTCGATGCAGTAGTTGTC
qRT-PCR-Elongation factor 1β-F:	GAATACGCTGCCAAGAAGTCAAA
qRT-PCR-Elongation factor 1β-R:	CCATCCATCTGAATACTGCGAAC

3. Results

3.1. Bacteria challenge

When the fat greenlings were infected with *V. harveyi*, fish from treatment group (TG) began to die on day 3 post-injection. No fish died in control group (CG) and no symptoms of *V. harveyi* was manifested,

Table 2
Summary of sequences analysis.

	Contig	Transcript	Unigene
Total Length (bp)	148023052	143347691	104039435
Sequence Number	481855	225279	189753
Max. Length (bp)	27018	27102	27102
Mean Length (bp)	307.19	636.31	548.29
N50 (bp)	391	951	672
GC%	51.88	52.44	51.99

Table 3
Quality of sequencing.

Sample	Raw Reads No.	Clean Reads No.	Clean Reads %	Q20%	GC %
TG_1	40,903,202	40,781,378	99.70	95.81	56.13
TG_2	44,024,372	43,793,566	99.47	93.20	55.74
TG_3	47,509,922	47,285,468	99.52	93.60	55.83
CG_1	43,586,686	43,466,468	99.72	95.48	55.80
CG_2	43,210,698	43,096,156	99.73	95.55	55.92
CG_3	43,520,556	43,415,678	99.75	95.87	55.95

Table 4
Annotation of unigenes in five different databases.

Database	Number of Unigenes	Percentage (%)
Annotated in NR	69508	36.63
Annotated in GO	42492	22.39
Annotated in KEGG	11766	6.2
Annotated in eggNOG	66616	35.11
Annotated in Swissprot	62559	32.97
Annotated in all database	8368	4.41
Total Unigenes	189753	100

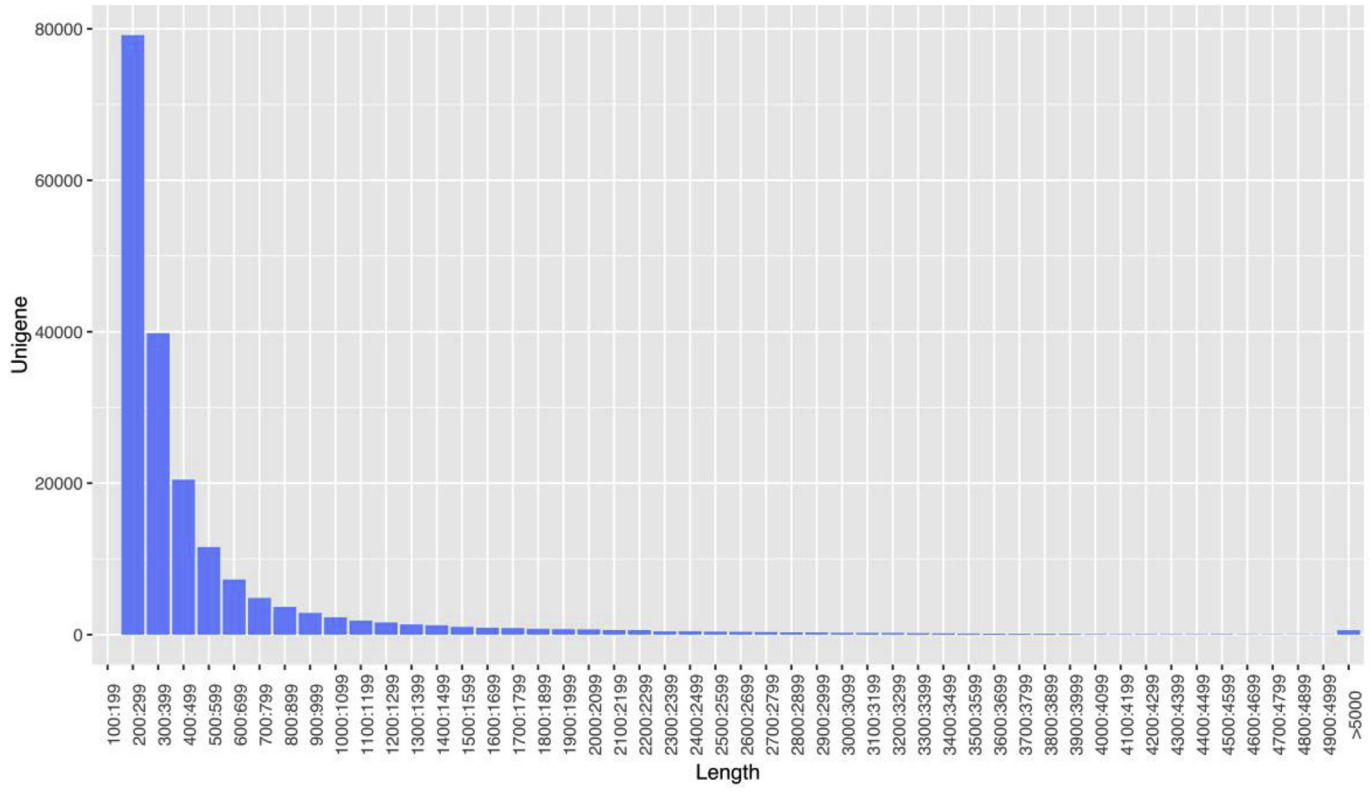

Fig. 1. The Length distribution of assembled unigenes. **X-axis:** unigene length, **Y-axis:** length frequency.

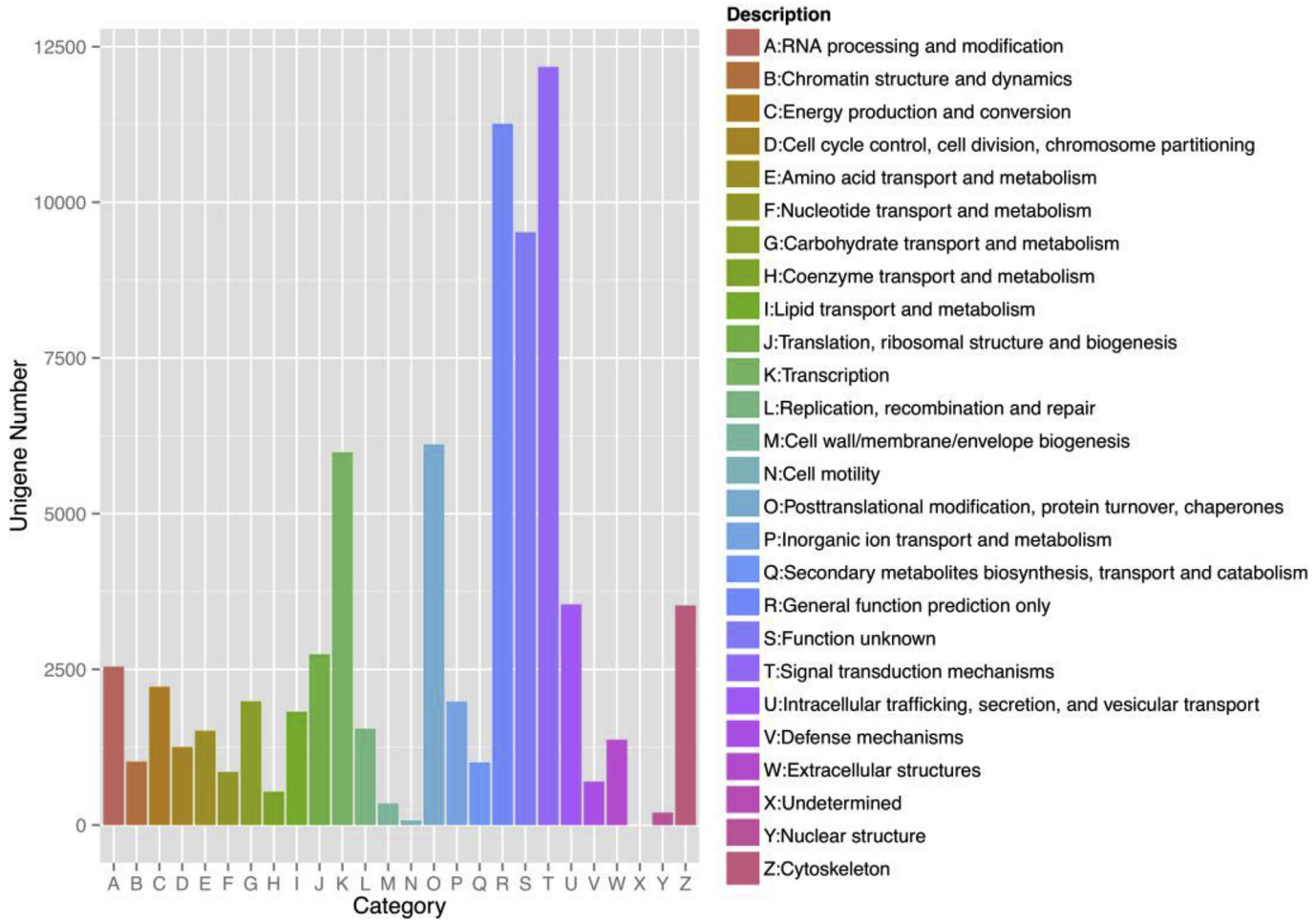

Fig. 2. The eggNOG classification of assembled unigenes. **X-axis:** the name of 26 categories in eggNOG, **Y-axis:** the number of unigene annotated in the category.

and randomly selected control fish were confirmed to be negative for *V. harveyi*. The infected fish exhibited typical clinical signs, including abdominal distension, exophthalmia and opacity of the eye, and peripheral hyperemia; and pure cultures of *V. harveyi* were re-isolated from liver, spleen, kidney and ascites in the moribund fat greenling.

3.2. Sequencing identify

To study immune response of fat greenling against *V. harveyi* infection, the spleen samples were collected from both control and treatment groups on day 3 post-injection, and three duplicates samples were sequenced using Illumina NextSeq500 platform for each group. After removing adaptors and low quality reads, the clean reads of infected and control groups were combined and used to draw the transcriptome information of fat greenling spleen. In total, there were 481855 contings and 225279 transcripts with an average length of 307 bp and 636 bp, respectively, after assembling the clean reads. A total of 189753 unigenes ranging from 200 bp to 27102bp (Fig. 1), with a N50 and mean length of 672bp and 548bp, respectively, were generated from 225279 transcripts (Table 2). The sequencing data of each treatment and control group have been deposited to NCBI sequence read archive database under the accession numbers SAMN10104598-SAMN10104603, respectively. The major characteristics of each library, including clean reads, error rate and GC content, are summarized in Table 3.

3.3. Functional annotation of unigenes

The sequences of unigenes were searched against five different databases. Totally, there were 8368 unigenes matched successfully in all five databases, accounting for 4.41% of the total unigenes (Table 4). The results showed that 69508 unigenes (36.63%) had successfully matched in the Nr database, and 62559 unigenes (32.97%) in Swissprot database (Table 4).

In eggNOG database, 66616 unigenes (35.11%) were successfully matched and divided into 26 descriptions. Among them, genes involved in signal transduction mechanisms, posttranslational modification, protein turnover, chaperones, and transcription were highly represented (Fig. 2).

For GO analysis, the genes were defined in three ontologies: biological process (BP), cellular component (CC) and molecular function (MF). In total, 42492 unigenes (22.39%) were successfully annotated in GO database and further assigned to 67 functional terms. In the BP category, those unigenes were mainly involved in metabolic process, cellular process, single-organism process and biological regulation. The CC category mainly consisted terms of cell, organelle and cell part were highly represented. In the MF category, unigenes involved in catalytic activity and binding were highly represented (Fig. 3).

Moreover, the orientation of unigenes in metabolic pathways was also analyzed using the KEGG database. The analysis showed that a total of 11766 unigenes (6.2%) were successfully annotated in KEGG database and assigned to five branches containing 35 known KEGG pathways. The percentages of unigenes in Metabolism, Genetic Information Processing, Environmental Information Processing,

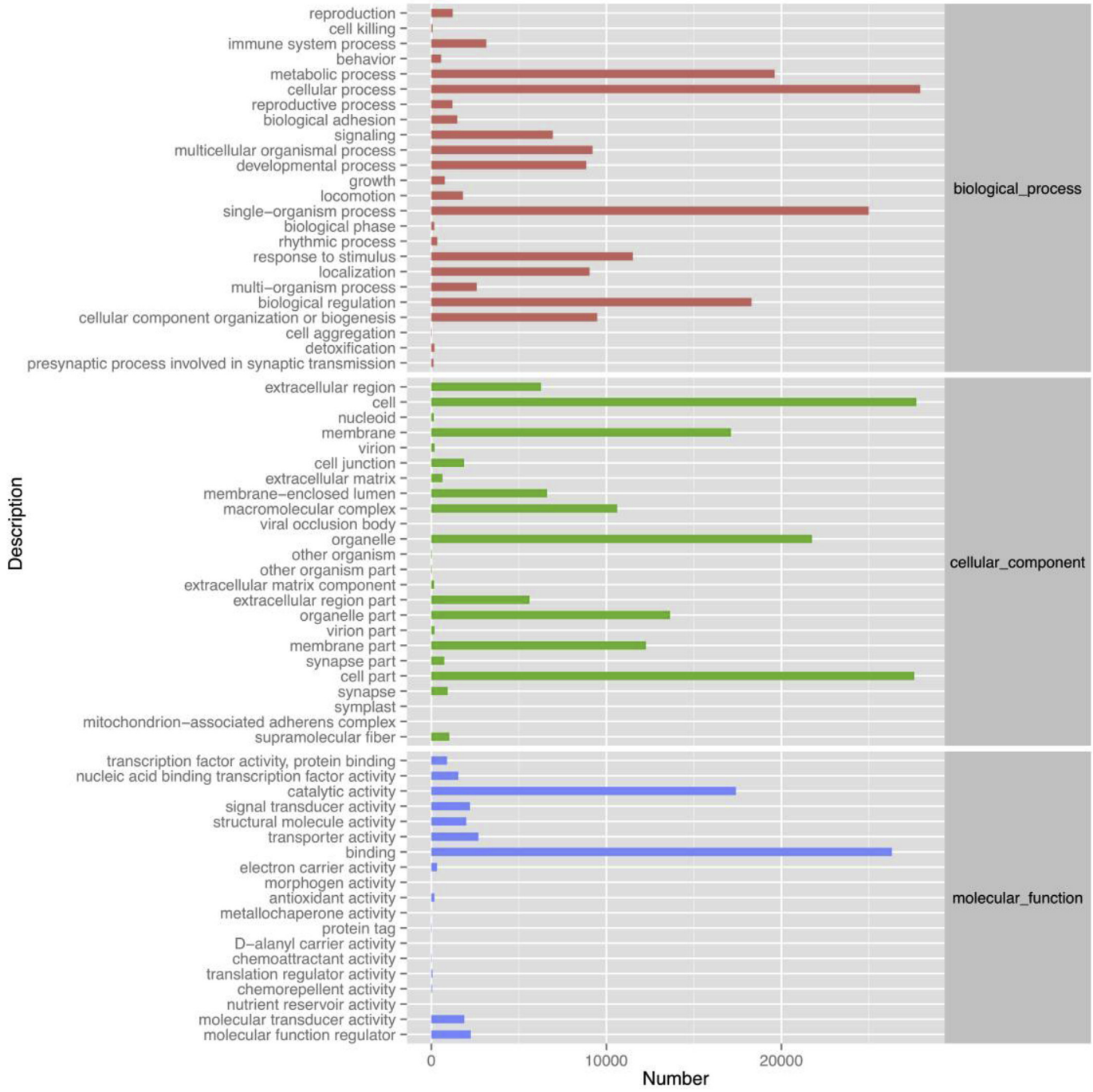

Fig. 3. GO classification of assembled unigenes. **X-axis:** three major functional categories of GO terms including biological process, cellular component and molecular function, **Y-axis:** the number of unigene annotated in the group.

Cellular Processes and Organismal Systems were 20.35%, 12.99%, 19.69%, 16.17% and 28.74%, respectively. Among the 35 KEGG pathways, the pathways involving homologs of the most unigenes were Signal transduction, Immune system, Endocrine system, Transport and catabolism, and Signaling molecules and interaction, which the numbers of unigenes in five pathways were 1644, 841, 736, 692 and 639, respectively (Fig. 4).

3.4. Identification and analysis of differentially expressed genes

The DEGs between *V. harveyi* infection and control groups were identified, and the results showed that a total of 5425 unigenes showed significantly differential expression in spleen following *V. harveyi* infection, which was about 2.86% of the total number of unigenes. Among them, the significantly up-regulated unigenes and down-regulated unigenes were 1837 and 3588, respectively (Fig. 5).

3.5. GO functional classification of DEGs

To understand the functions of DEGs, all DEGs were mapped against GO database and subjected to enrichment analysis. GO analysis showed that DEGs were classified into three major functional categories containing 307 GO terms based on the criteria of p-value ≤ 0.05. The numbers of GO terms in BP category, CC category and MF category were 192, 68 and 47, respectively. The Fig. 6 showed the top 10 GO terms with the most abundant DEGs in MF category, CC category and

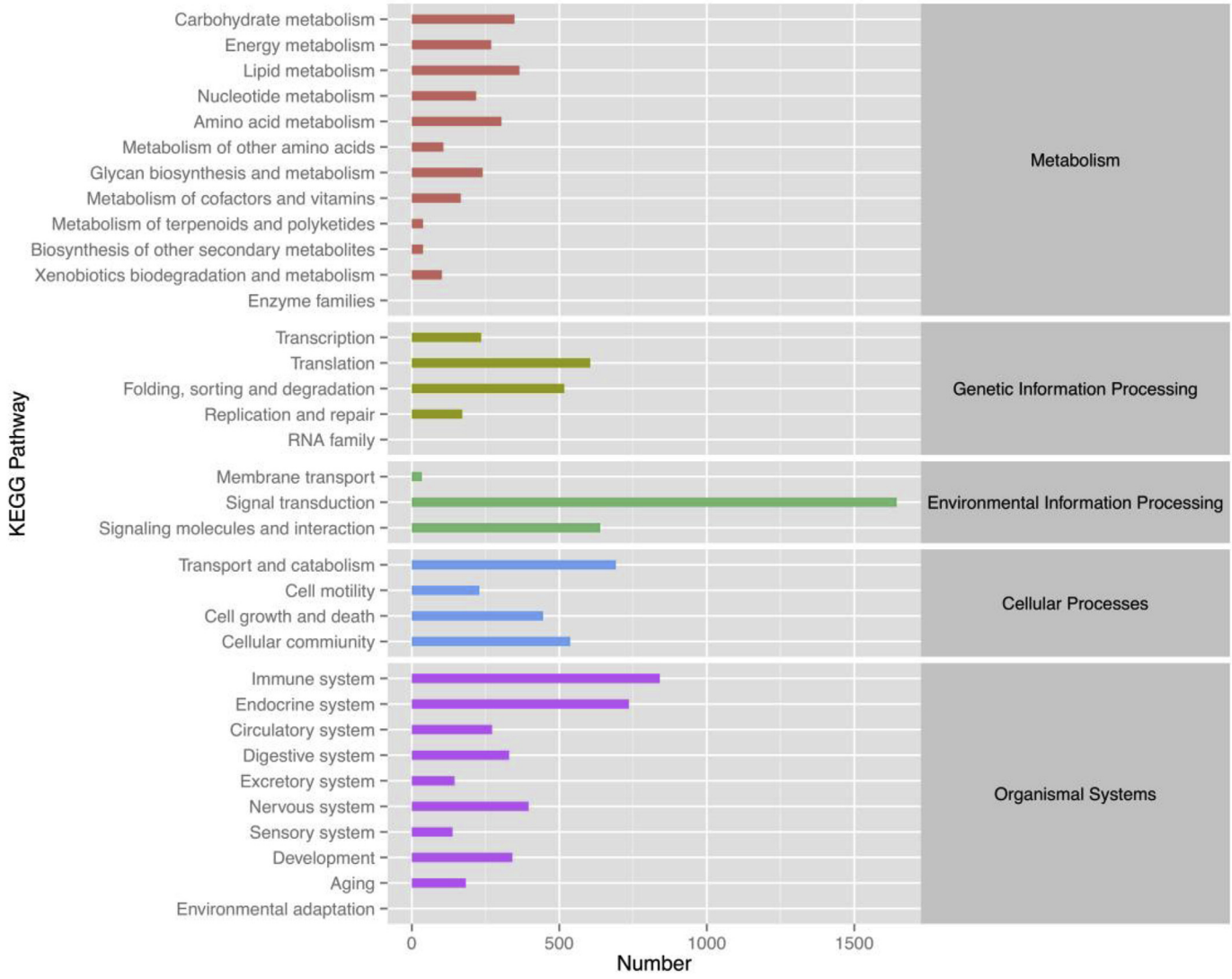

Fig. 4. KEGG classification of assembled unigenes. **X-axis:** the number of unigene annotated in the group, **Y-axis:** five major categories including metabolism, genetic information processing, environmental information processing, cellular processes and organismal systems.

BP category, respectively. In MF category, the DEGs were significantly enriched in the term of catalytic activity, RNA binding and oxidoreductase activity; in CC category, the DEGs were significantly enriched in the term of intracellular part, organelle and membrane – bounded organelle; in BP category, the DEGs were significantly enriched in the term of metabolic process, organic substance metabolic process and primary metabolic process.

3.6. Pathway classification enrichment of DEGs

To perform functional classification and pathway assignment of fat greenling genes after *V. harvey*i infection, all DEGs were analyzed against the KEGG database. After mapping to the KEGG database, the results showed that the 714 DEGs were successfully annotated and assigned to 207 pathways. Among them, a total of 42 pathways were significantly enriched (corrected p-value ≤ 0.05) in pathways categorized in three branches, including genetic information processing, metabolism and organismal systems, of which the DEGs enriched in metabolism were dominant. The top 20 of pathways with most abundant DEGs involved in *V. harvey*i infection were shown in Fig. 7, including ubiquinone and other terpenoid-quinone biosynthesis, tyrosine metabolism, and tryptophan metabolism and so on. Among them, the number of genes involved in complement and coagulation cascades, ribosome, oxidative phosphorylation and peroxisome proliferator-activated receptor (PPAR) signaling pathway were most abundant. The genes involved in these five pathways were shown in Table 5.

3.7. Validation of the different expression genes by qRT-PCR

The relative mRNA expression level of 12 genes, including 6 up-regulated and 6 down-regulated genes, were randomly selected for qRT-PCR analysis to validate the reliability of DEGs data. As shown in Fig. 8, the expression levels of 12 genes analyzed by qRT-PCR were mainly agreement with the data of RNA-seq. The qRT-PCR analysis results therefore confirmed that the data of RNA-seq were reliable.

4. Discussion

Fat greenling is one of the most commercial aquatic animal species, but its farming has been severely damaged by vibriosis caused by *V. harvey*i infection [1,2]. The fish spleen is an important tissue associated with immune responses, playing a crucial role in combating bacterial infection. Many studies have been performed to analyzed interaction of bacteria and host on 1dpi and 2dpi using transcriptome sequencing, but few reports focused on interaction of bacteria and host on 3dpi [15,16]. Thus, the transcriptome profiling of fat greenling spleen on 3dpi in this

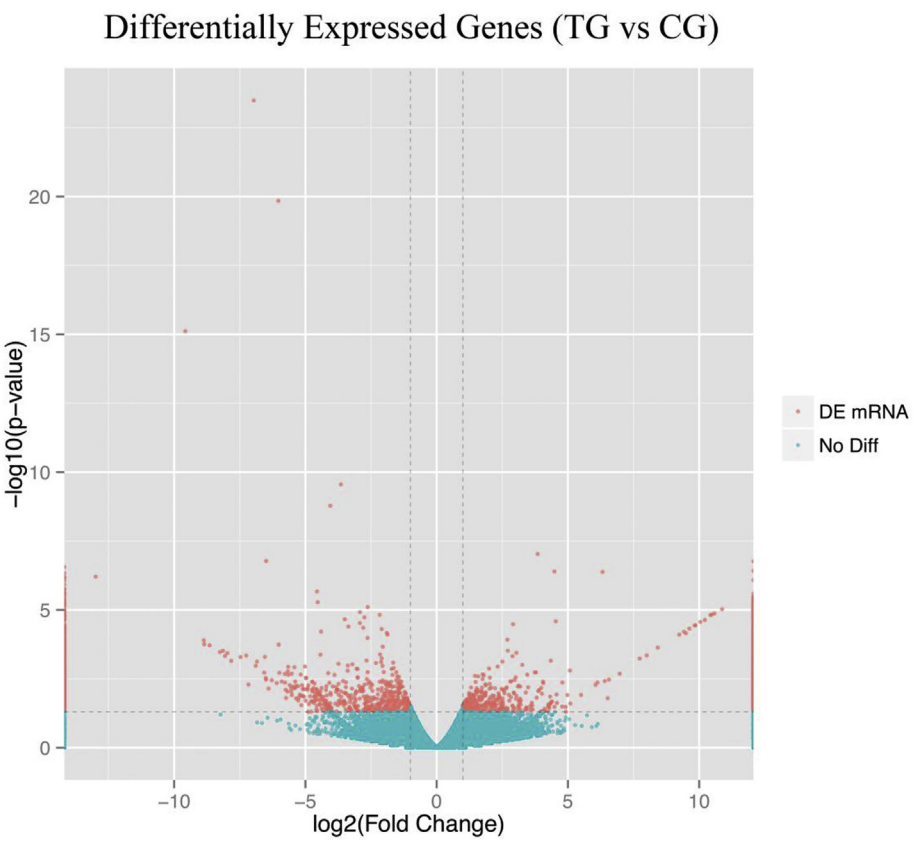

Fig. 5. Volcano Plot of differently expressed genes between *V. harveyi* infected and non-infected fat greenling. The vertical line is twice of the difference threshold, and horizontal line represents *p*-value ¼ 0.05. Red dots represent the significant differential expression genes (*p*-value adjusted for multiple testing < 0.05). (For interpretation of the references to color in this figure legend, the reader is referred to the Web version of this article.)

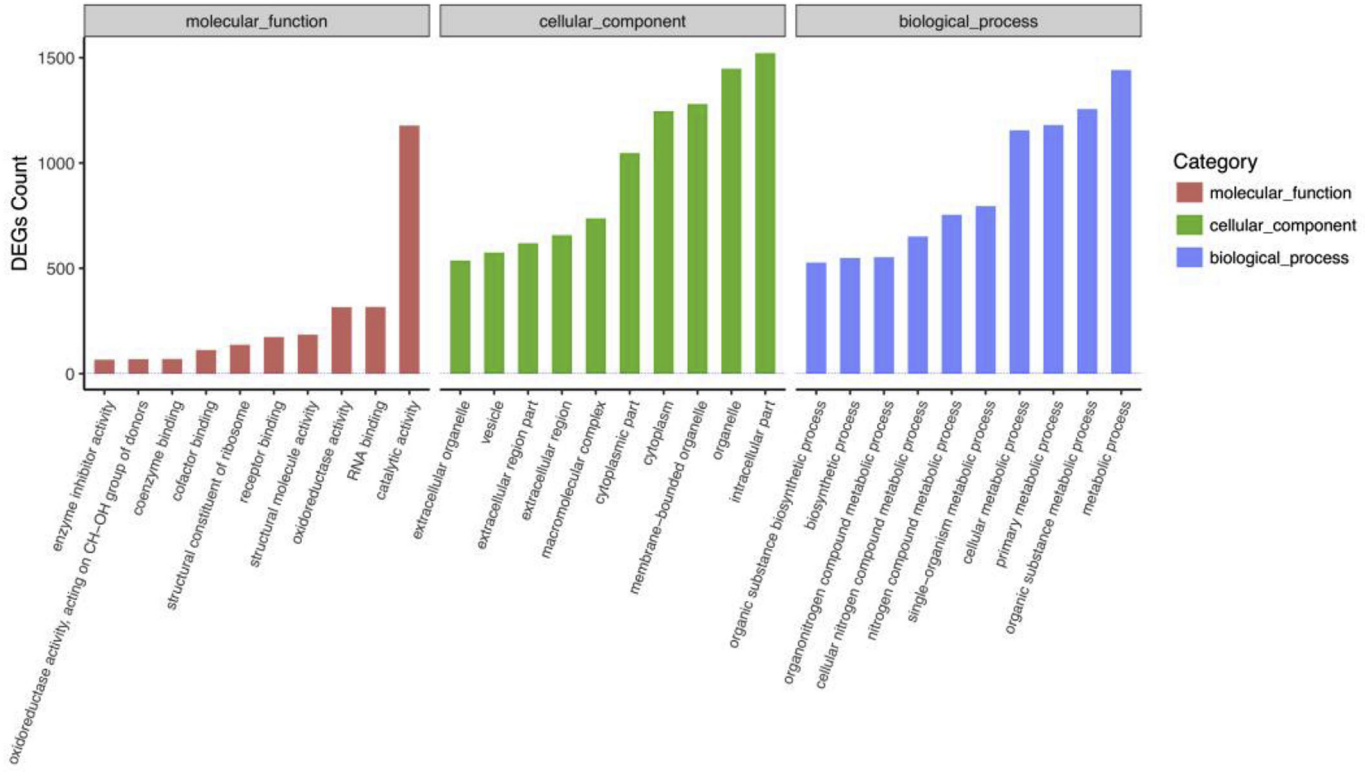

Fig. 6. Gene ontology (GO) classifications of differentially expressed genes (DEGs). **X-axis:** three major functional categories of GO terms including biological process, cellular component and molecular function, **Y-axis:** the numbers of DEGs.

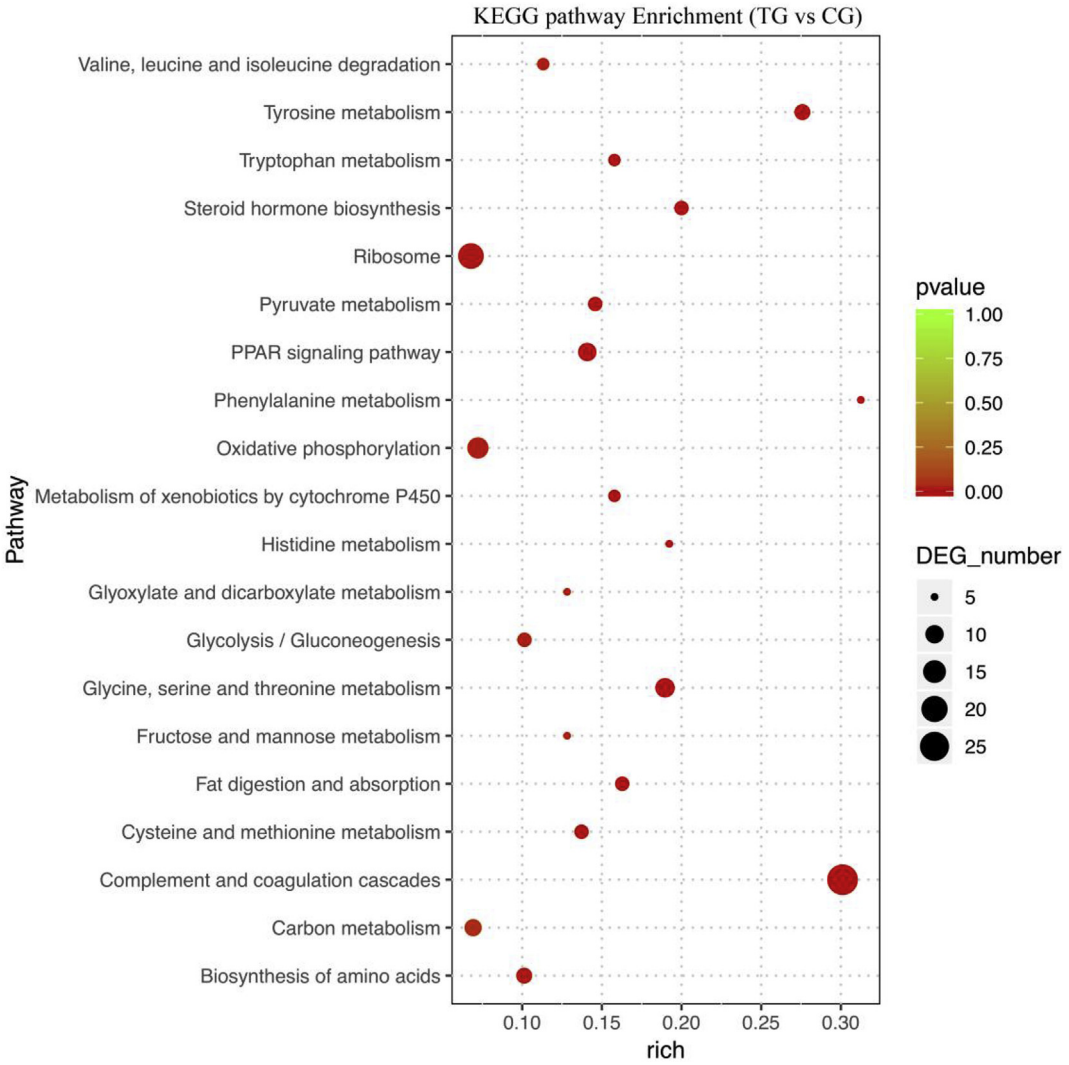

Fig. 7. Scatterplot of enriched KEGG pathways for differentially expressed genes (DEGs). **X-axis:** the percentages of DEGs belong to the corresponding pathway, **Y-axis:** the top 20 pathways. The sizes of bubble represent the number of DEGs in the corresponding pathway, and the colors of the bubble represent the enrichment *p*-value of the corresponding pathway. (For interpretation of the references to color in this figure legend, the reader is referred to the Web version of this article.)

paper will promote the understanding of *V. harvey*i-host interactions and identify abundant immune-related genes in response to *V. harvey*i infection.

To date, little information about the genetic sequence of fat greenling is reported. The research on transcriptome profiling of fat greenling was first carried out in the present study. A total of 189753 unigenes were obtained with an N50 of 672 bp by transcriptome profiling. These information enriched our understanding of the fat greenling genes, which also provided abundant data for the future study of fat greenling.

Genes that interact with each other play an important role in generating a response to bacteria infection. The first step of bacterial infection process is attaching to a cell surface, and usually require modification of host cellular junction to gain access for invasion [28]. Previous studies have shown that a large number of genes that are related to TLR signaling pathway, chemokine signaling pathway, antigen processing and presentation cell-cell junction were significantly differentially expressed on 1dpi and 2dpi [15,16], and most of these genes are connected with the recognition of pathogenic bacteria. In this paper, we focused on the DEGs on 3dpi of *V. harveyi* in fat greenling. GO enrichment analysis showed that the DEGs in fat greenling spleen on 3dpi were significantly enriched in the term of catalytic activity, RNA binding and oxidoreductase activity in CC category, which were correlated with inflammatory responses. KEGG analysis showed that the DEGs were mainly involved in complement and coagulation cascades, ribosome, oxidative phosphorylation, glycine, serine and threonine metabolism and PPAR signaling pathway on 3dpi. Those pathways were also mainly associated with inflammatory responses, immune regulation, and immune clearance, rarely involved in bacterial adhesion and pathogen identification. Those results suggested that the host may have completed the identification of the pathogen on 3dpi, and the interaction of bacteria and host might begin to new phase of elimination of bacteria through inflammatory response. As discussed below, several important KEGG pathways were highlighted, which were likely involved in mediating fat greenling response against *V. harveyi* infection.

Complement and coagulation cascades. The complement system is an important part of the innate immunity, playing a vital role in immune surveillance and immune clearance [29]. Previous studies have shown that there are three distinct pathways responsible for target recognition and formation of a protease complex, including the classical pathway, the lectin pathway and the alternative pathway, and C3 is a core component for activation of the complement system by the three pathways [30,31]. In our results, many complement molecules were significantly higher expressed, including C1r, C1q, C3, C4a, C8α, C8γ, C9 and some complement factor, and the changes of gene expression of

Table 5
The differentially expression genes involved in five key KEGG pathways.

Cenes	Species	Log_2FC	*p*-value
Complement and coagulation cascades			
Complement C3	*Bos taurus*	20.30	$8.62E^{-07}$
Fibrinogen β	*Bos grunniens mutus*	20.21	$1.21E^{-06}$
Vitronectin isoform 5	*Pan troglodytes*	19.35	$3.67E^{-06}$
Fibrinogen alpha chain	*Trichechus manatus latirostris*	19.18	$4.22E^{-06}$
Plasminogen-like isoform 1	*Odobenus rosmarus divergens*	18.71	$1.03E^{-05}$
Prothrombin-like	*Ailuropoda melanoleuca*	18.60	$9.60E^{-06}$
Plasma protease C1 inhibitor isoform 1	*Pan troglodytes*	18.28	$1.34E^{-05}$
Complement factor B	*Ovis aries*	18.12	$1.73E^{-05}$
Antithrombin-III-like	*Loxodonta africana*	18.04	$2.30E^{-05}$
Complement C1r Subcomponent-like	*Ailuropoda melanoleuca*	18.00	$2.11E^{-05}$
Vitamin K-dependent protein C	*Tursiops truncatus*	17.35	$4.23E^{-05}$
Complement C4-A-like	*Bos taurus*	8.83	$1.77E^{-04}$
Heparin cofactor 2	*Equus caballus*	16.72	$1.27E^{-04}$
Hypothetical protein PANDA	*Ailuropoda melanoleuca*	8.24	$3.37E^{-04}$
Complement C8 γ	*Felis catus*	16.65	$1.23E^{-04}$
Complement factor H-related protein 2	*Dasypus novemcinctus*	16.23	$3.16E^{-04}$
Complement C1q subunit C isoform	*Orcinus orca*	16.04	$3.39E^{-04}$
Complement C1q subunit C isoform 3	*Orcinus orca*	15.42	$1.69E^{-03}$
Complement C1q subunit B	*Pan troglodytes*	15.29	$7.26E^{-04}$
Complement C8B	*Sus scrofa*	15.21	$7.05E^{-04}$
Complement C1q subunit A	*Pteropus alecto*	15.09	$2.11E^{-03}$
Complement C9	*Odobenus rosmarus divergens*	14.84	$1.25E^{-03}$
Complement C8α	*Loxodonta africana*	14.45	$3.33E^{-03}$
Complement factor	*Bos taurus*	14.19	$2.75E^{-03}$
Coagulation factor VII isoform 1	*Odobenus rosmarus divergens*	13.86	$7.49E^{-03}$
Mannose-binding protein A-like	*Orcinus orca*	13.61	$8.19E^{-03}$
Kininogen-2 isoform 3	*Orcinus orca*	13.61	$5.19E^{-03}$
Complement 2 precursor	*Bos taurus*	13.57	$5.05E^{-03}$
Ribosome			
ribosomal protein S20	*Coregonus maraena*	1.46	$1.74E^{-02}$
Ribosomal protein L27a	*Bos taurus*	17.27	$7.82E^{-05}$
40S ribosomal protein S12	*Tupaia chinensis*	1.76	$2.09E^{-02}$
acidic ribosomal phosphoprotein P1	*Homo sapiens*	17.16	$5.75E^{-05}$
40S ribosomal protein S28	*Tursiops truncatus*	16.52	$1.60E^{-04}$
60S acidic ribosomal protein P2	*Trichechus manatus latirostris*	16.43	$1.46E^{-04}$
40S ribosomal protein S21-like isoform 1	*Otolemur garnettii*	4.38	$6.82E^{-03}$
40S ribosomal protein S21-like isoform 2	*Otolemur garnettii*	2.63	$1.05E^{-04}$
40S ribosomal protein S26	*Trichechus manatus latirostris*	3.46	$6.33E^{-03}$
60S ribosomal protein L24	*Otolemur garnettii*	1.61	$3.06E^{-02}$
60S ribosomal protein L34	*Bos grunniens mutus*	4.88	$5.42E^{-03}$
60S ribosomal protein L26-like	*Callithrix jacchus*	3.01	$1.39E^{-03}$
hypothetical protein LOC100725823	*Cavia porcellus*	5.60	$5.38E^{-03}$
40S ribosomal protein S20-like	*Rattus norvegicus*	15.01	$1.41E^{-03}$
40S ribosomal protein S20-like	*Rattus norvegicus*	2.09	$6.85E^{-03}$
hypothetical protein M91_00440	*Bos grunniens mutus*	3.95	$5.99E^{-03}$
hypothetical protein EGK_07538	*Macaca mulatta*	13.17	$7.78E^{-03}$
28S ribosomal protein S21, mitochondrial-like	*Monodelphis domestica*	4.20	$2.62E^{-02}$
39S ribosomal protein L18	*Canis lupus familiaris*	12.45	$1.76E^{-02}$
Oxidative phosphorylation			
NADH dehydrogenase subunit 2	*Cottus reinii*	−1.13	$2.24E^{-02}$
ATP synthase subunit epsilon	*Sus scrofa*	2.52	$6.52E^{-03}$
Cytochrome c oxidase subunit 4 isoform 1	*Pteropus alecto*	14.70	$1.30E^{-03}$
succinate dehydrogenase iron-sulfur subunit	*Orcinus orca*	14.51	$3.21E^{-03}$
NADH dehydrogenase-like	*Oryctolagus cuniculus*	14.03	$3.10E^{-03}$
NADH dehydrogenase1β subcomplex subunit 9	*Bos taurus*	2.40	$1.48E^{-02}$
NADH dehydrogenase Fe-S protein 7	*Homo sapiens*	3.62	$1.41E^{-02}$
cytochrome b-c1 complex subunit 8-like isoform 1	*Felis catus*	12.68	$1.77E^{-02}$
NADH dehydrogenase1α subcomplex subunit 1	*Canis lupus familiaris*	12.68	$2.50E^{-02}$
cytochrome c oxidase polypeptide 7A2	*Oryctolagus cuniculus*	12.61	$2.61E^{-02}$
cytochrome c oxidase copper chaperone-like	*Cavia porcellus*	12.61	$1.70E^{-02}$
NADH dehydrogenase1α subcomplex subunit 6-like	*Equus caballus*	12.27	$2.88E^{-02}$
ATP synthase-coupling factor 6	*Bos taurus*	12.16	$3.23E^{-02}$
Glycine, serine and threonine metabolism			
5-aminolevulinate synthase	*Orcinus orca*	15.79	$4.21E^{-04}$
glycine N-methyltransferase	*Odobenus rosmarus divergens*	15.38	$6.70E^{-04}$
serine–pyruvate aminotransferase	*Felis catus*	15.16	$9.75E^{-04}$
unnamed protein product	*Tetraodon nigroviridis*	−1.14	$4.87E^{-02}$
glyoxylate reductase	*Bos taurus*	14.70	$1.34E^{-03}$
Glycine amidinotransferase	*Pteropus alecto*	14.55	$2.04E^{-03}$
glycerate kinase isoform 1	*Ovis aries*	14.36	$2.56E^{-03}$

(*continued on next page*)

Table 5 (*continued*)

Cenes	Species	Log_2FC	*p*-value
serine hydroxymethyltransferase	*Equus caballus*	4.93	$6.97E^{-03}$
alanine–glyoxylate aminotransferase 2	*Bos taurus*	14.06	$4.12E^{-03}$
Serine dehydratase-like protein	*Myotis davidii*	13.17	$8.02E^{-03}$
L-threonine dehydratase catabolic TdcB-like	*Strongylocentrotus purpuratus*	−13.89	$4.09E^{-03}$
PPAR signaling pathway			
angiopoietin-related protein 4-like	*Maylandia zebra*	1.38	$2.51E^{-02}$
Angiopoietin-related protein 4 precursor	*Salmo salar*	1.08	$2.10E^{-02}$
fatty acid-binding protein	*Canis lupus familiaris*	15.46	$8.06E^{-04}$
Sterol 26-hydroxylase	*Myotis davidii*	16.40	$1.72E^{-04}$
Fatty acid-binding protein	*Salmo salar*	1.01	$2.96E^{-02}$
Fatty acid desaturase 2	*Bos grunniens mutus*	14.40	$1.89E^{-03}$
apolipoprotein A-I	*Tursiops truncatus*	19.80	$1.71E^{-06}$
phosphoenolpyruvate carboxykinase	*Odobenus rosmarus divergens*	7.95	$3.66E^{-04}$
acyl-CoA-binding protein isoform 1	*Felis catus*	6.48	$3.34E^{-03}$
unnamed protein product	*Oikopleura dioica*	−12.11	$3.76E^{-02}$

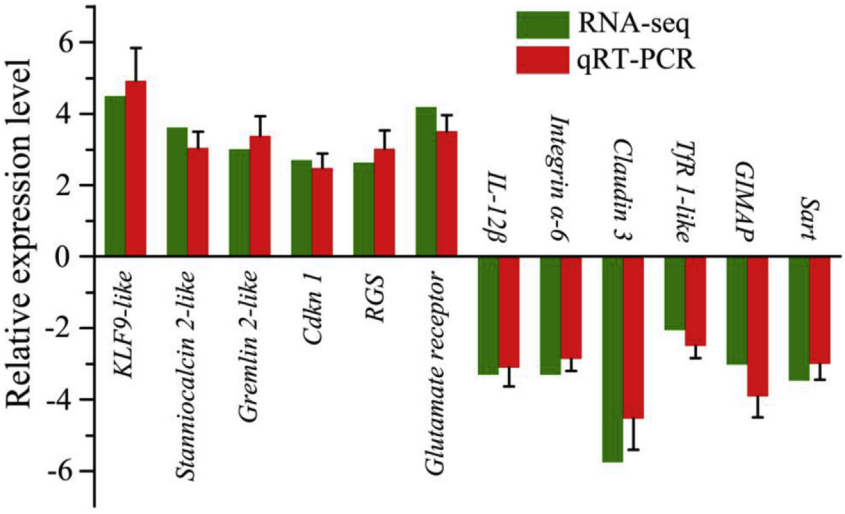

Fig. 8. Validation of RNA-seq data by qRT-PCR analysis. **X-axis:** gene name, **Y-axis:** the relative expression level was expressed as log2 (fold change) in gene expression. The relative expression of 12 random genes, were determined by RT-qPCR (red column) and compared with the results of RNA-seq (green column). Error bars represented standard deviation (SD) (n = 3). (For interpretation of the references to color in this figure legend, the reader is referred to the Web version of this article.)

C3 was the largest in complement molecules, suggesting that the complement system of fat greenling was activated after *V. harvey*i infection. Similarly, trancriptome profiles analysis show that the complement system also play defense roles as an innate immune response to protect amur sturgeon (*Acipenser schrenckii*) against *Yersinia ruckeri* invasion [32]. The regulation of the complement system of fat greenling against *V. harvey*i infection remains to be explained in the future.

Ribosome. Ribosome is protein synthesis site, playing an important role in biological activities. We found that many 40S ribosomal protein subunits and 60S ribosomal protein subunits were significantly higher expressed after *V. harvey*i infection in this paper, suggesting host might accelerate the efficiency of protein synthesis in order to resist bacterial infection. In addition, the dsRNA-activated protein kinase (PKR) is capable of driving apoptosis, and previous studies shows that the kinase is primarily localized in free 40S ribosomal subunit [33–35]. Therefore, we guessed that the up-regulation of expressions of 40S ribosomal subunit may be also to promote apoptosis to killing the infected cells.

Oxidative phosphorylation. In this study, many NADH dehydrogenase genes were also significantly higher expressed, and these genes were enriched to oxidative phosphorylation pathway. NADPH oxidase system is pivotal regulators of polymorphonuclear phagocytosis, playing an important role in innate immunity [36]. The polymorphonuclear phagocytosis may be compromised by defects in the NADPH oxidase system, which impair the respiratory burst and intracellular bactericidal ability [37,38]. Thus, the activation of oxidative phosphorylation pathway suggested that host might begin to kill the bacterium by phagocytosis.

Glycine, serine and threonine metabolism. The enhancement of metabolome could improve the anti-infection ability of the host, and pattern recognition analysis has shown that serine metabolism of survival host is significantly higher than that of dying [39]. It also has been reported that amino acids can promote innate immunity [40,41]. Moreover, exogenous l-leucine and l-serine could enhance the immunity to eliminate *Streptococcus iniae* by up-regulated of glycine, serine and threonine metabolism to improve phagocytic activity in tilapias (*Oreochromis mossambic*us) [39]. This research also showed that glycine, serine and threonine metabolism was also enhanced after *V. harvey*i infection, which might play defense roles in improving innate immunity to protect fat greenling against pathogen invasion.

PPAR signaling pathway. The PPAR signaling pathway were involved in inflammation, lipid metabolism, mitochondrial biogenesis, and maintenance of metabolic homeostasis [42,43]. Many genes belonging to the PPAR signaling pathway were significantly up-regulated in present study, and these genes were mainly related to lipid metabolism, such as fatty acid-binding protein, sterol 26-hydroxylase and fatty acid desaturase 2. The lipid metabolism pathways, like PPAR signaling pathway, could controll immune cell activation by influencing PM lipid raft composition [44]. Previous study also show that PPAR molecules could modulate the NF-κB and Nrf2/CREB signaling pathways to enhance anti-inflammatory effects [45,46]. In this paper, the expression of NF-κB and Nrf2 were also significantly higher expressed, suggesting the host may activate the inflammatory response to resist the bacterial invasion.

In summary, we conducted a comparative analysis of mRNA

expression of fat greenling spleen following *V. harvey*i challenge by transcriptomics. A total of 5425 genes were found to be differentially expressed. Further annotation and analysis indicated that DEGs mainly enriched in five main pathways involving in the host immune response to bacterial infection, which mainly associated with phagocytosis and pathogen clearance, suggesting that the host might begin to clear and kill the invading bacteria on 3dpi. These results are the primary research about the anti-microbial immune response of fat greenling, which will provide potential directions and resource to the further research about the fat greenling.

Acknowledgements

This study was supported by Key Project of Research and Development Plan of Shandong Province (2016CYJS04A01-3; 2018GHY115033; 2017GHY15109) and Key Project of Agricultural Applied Technology Research of Shandong Province.

References

[1] F. Hu, L. Pan, F. Gao, Y. Jian, X. Wang, L. Li, et al., Effect of temperature on incubation period and hatching success of fat greenling (*hexagrammos otakii*, Jordan & Starks) eggs, Aquacult. Res. 48 (2017) 361–365.
[2] K.A. Habib, D. Jeong, J.G. Myoung, S.K. Min, Y.S. Jang, J.S. Shim, et al., Population genetic structure and demographic history of the fat greenling *Hexagrammos otakii*, Genes. Genom. 33 (2011) 413–423.
[3] C.M. Feng, H.L. Jing, Y. Li, Q. Li, H. Li, A pathogen and treatment of fat greenling *Hexagrammos otakii* with streptococcal disease, J. Dalian Fish. Univ. 25 (2010) 270–274.
[4] O.L. Haenen, Z.E. Van, R. Jansen, I. Roozenburg, M.Y. Engelsma, A. Dijkstra, S.A. Boers, M. Voorbergen-Laarman, A.V.M. Möller, *Vibrio vulnificus* outbreaks in Dutch eel farms since 1996: strain diversity and impact, Dis. Aquat. Org. 108 (2014) 201–209.
[5] H.T. Dong, S. Taengphu, P. Sangsuriya, W. Charoensapsri, K. Phiwsaiya, T. Sornwatana, P. Khunrae, T. Rattanarojpong, S. Senapin, Recovery of *vibrio harveyi* from scale drop and muscle necrosis disease in farmed barramundi, *lates calcarifer*, in Vietnam, Aquaculture 473 (2017) 89–96.
[6] A. Rønneseth, D. Castillo, P. D'Alvise, Tønnesen, G. Haugland, T. Grotkjær, K. Engell-Sørensen, L. Nørremark, Bergh, H.I. Wergeland, L. Gram, Comparative assessment of vibrio virulence in marine fish larvae, J. Fish. Dis. 40 (2017) 1373.
[7] R. Srinivasan, S. Santhakumari, A.V. Ravi, In vitro antibiofilm efficacy of *Piper betle* against quorum sensing mediated biofilm formation of luminescent *Vibrio harveyi*, Microb. Pathog. 110 (2017) 232–239.
[8] H.T. Nguyen, T.T.T. Nguyen, Y.T. Wang, P.C. Wang, S.C. Chen, Effectiveness of formalin-killed vaccines containing CpG oligodeoxynucleotide 1668 adjuvants against *Vibrio harveyi* in orange-spotted grouper, Fish Shellfish Immunol. 68 (2017) 124–131.
[9] X. Zhang, B. Austin, Pathogenicity of *Vibrio harveyi* to salmonids, J. Fish. Dis. 23 (2000) 93–102.
[10] T. Kraxberger-Beatty, D. McGarey, H. Grier, D. Lim, *Vibrio harveyi*, an opportunistic pathogen of common snook, *Centropomus undecimalis* (Bloch), held in captivity, J. Fish. Dis. 13 (1990) 557–560.
[11] K.M. Won, S.I. Park, Pathogenicity of *Vibrio harveyi* to cultured marine fishes in Korea, Aquaculture 285 (2008) 8–13.
[12] C. Wang, C. Zhao, M. Fu, W. Bao, L. Qiu, Molecular cloning, characterization and expression analysis of Toll-like receptor 5M gene in Japanese sea perch (*Lateolabrax japonicas*) after bacterial infection, Fish Shellfish Immunol. 56 (2016) 199–207.
[13] G. Biswas, S. Bilen, T. Kono, M. Sakai, J. Hikima, Inflammatory immune response by lipopolysaccharide-responsive nucleotide binding oligomerization domain (NOD)-like receptors in the Japanese pufferfish (*Takifugu rubripes*), Dev. Comp. Immunol. 55 (2016) 21–31.
[14] C. Zhou, H. Lin, Z. Huang, J. Wang, Y. Wang, W. Yu, Cloning and expression analysis of c-type lysozyme gene in golden pompano, *Trachinotus ovatus*, Fish Shellfish Immunol. 54 (2016) 580–585.
[15] Y.L. Jiang, S.S. Feng, S.H. Zhang, H. Liu, J.X. Feng, X.D. Mu, et al., Transcriptome signatures in common carp spleen in response to *Aeromonas hydrophila* infection, Fish Shellfish Immunol. 57 (2016) 41–48.
[16] S. Maekawa, O. Byadgi, Y.C. Chen, T. Akoi, H. Takeyama, T. Yoshida, et al., Transcriptome analysis of immune response against Vibrio harveyi infection in orange-spotted grouper (*Epinephelus coioides*), Fish Shellfish Immunol. 70 (2017) 628–637.
[17] D.H. Ahn, S. Kang, H. Park, Transcriptome analysis of immune response genes induced by pathogen agonists in the Antarctic bullhead notothen *Notothenia coriiceps*, Fish Shellfish Immunol. 55 (2016) 315–322.
[18] J. Jiang, M. Miyata, C. Chan, S.Y. Ngoh, W.C. Liew, J.M. Saju, et al., Differential transcriptomic response in the spleen and head kidney following vaccination and infection of Asian seabass with *Streptococcus iniae*, PloS One 9 (2014) e99128.
[19] J. Zhu, C. Li, Q. Ao, Y. Tan, Y. Luo, Y. Guo, et al., Trancriptomic profiling revealed the signatures of acute immune response in tilapia (*Oreochromis niloticus*) following Streptococcus iniae challenge, Fish Shellfish Immunol. 46 (2015) 346–353.
[20] R. Zhang, L.L. Zhang, X. Ye, Y.Y. Tian, C.F. Sun, M.X. Lu, et al., Transcriptome profiling and digital gene expression analysis of Nile tilapia (*Oreochromis niloticus*) infected by Streptococcus agalactiae, Mol. Biol. Rep. 40 (2013) 5657–5668.
[21] S.F. Altschul, W. Gish, W. Miller, E.W. Myers, D.J. Lipman, Basic local alignment search tool, J. Mol. 215 (1990) 403–410.
[22] B. Li, C.N. Dewey, RSEM: accurate transcript quantification from RNA-Seq data with or without a reference genome, BMC Bioinf. 12 (2011) 323.
[23] C. Trapnell, B.A. Williams, G. Pertea, A. Mortazavi, G. Kwan, M.J. van Baren, et al., Transcript assembly and quantification by RNA-Seq reveals unannotated transcripts and isoform switching during cell differentiation, Nat. Biotechnol. 28 (2010) 511–515.
[24] S. Anders, W. Huber, Differential expression analysis for sequence count data, Genome Biol. 11 (2010) R106.
[25] Y. Benjamini, Y. Hochberg, Controlling the false discovery rate: a practical and powerful approach to multiple testing, J. R. Stat. Soc. Ser. B. 57 (1995) 289–300.
[26] X. Mao, T. Cai, J.G. Olyarchuk, L. Wei, Automated genome annotation and pathway identification using the KEGG Orthology (KO) as a controlled vocabulary, Bioinformatics 21 (2005) 3787–3793.
[27] F.G. Liu, X.Q. Tang, X.Z. Sheng, J. Xing, W.B. Zhan, *Edwardsiella tarda* outer membrane protein C: an Immunogenic protein induces highly protective effects in flounder (*Paralichthys olivaceus*) against edwardsiellosis, Int. J. Mol. Sci. 17 (2016) 1–13.
[28] J.A. Guttman, B.B. Finlay, Tight junctions as targets of infectious agents, Biochim. Biophy. acta 1788 (2009) 832–841.
[29] M.C. Carroll, The complement system in regulation of adaptive immunity, Nat. Immunol. 5 (2004) 981–986.
[30] M. Nakao, M. Tsujikura, S. Ichiki, T.K. Vo, T. Somamoto, The complement system in teleost fish: progress of post-homolog-hunting researches, Dev. Comp. Immunol. 35 (2011) 1296–1308.
[31] H.M. Claire H, L. John D, The complement system in teleosts, Fish Shellfish Immunol. 12 (2002) 399–420.
[32] S.W. Li, Y. Zhang, Y.S. Cao, D. Wang, H.B. Liu, T.Y. Lu, et al., Trancriptome profiles of Amur sturgeon spleen in response to *Yersinia ruckeri* infection, Fish Shellfish Immunol. 70 (2017) 451–460.
[33] H.K. Bae, J. Shinozuka, Z. Islam, J.J. Pestka, Satratoxin G interaction with 40S and 60S ribosomal subunits precedes apoptosis in the macrophage, Toxicol. Appl. Pharmacol. 237 (2009) 137–145.
[34] H.K. Bae, J.J. Pestka, Deoxynivalenol induces p38 interaction with the ribosome in monocytes and macrophages, Toxicol. Sci. 105 (2008) 59–66.
[35] J.J. Pestka, Mechanisms of deoxynivalenol-induced gene expression and apoptosis, Food Addit. Contam. 24 (2008) 1–13.
[36] S.R. Yan, R. Bortolussi, T.B. Issekutz, A.C. Issekutz, Increased chemoattractant induced neutrophil oxidative burst, accelerated apoptosis, and dysregulated tyrosine phosphorylation associated with lifelong bacterial infections, Clin. Immunol. 117 (2005) 36–47.
[37] G. Cicchetti, P.G. Allen, M. Glogauer, Chemotactic signaling pathways in neutrophils: from receptor to actin assembly, Crit. Rev. Oral Biol. Med. 13 (2002) 220–228.
[38] G. Berton, Tyrosine kinases in neutrophils, Curr. Opin. Hematol. 6 (1999) 51–58.
[39] C.C. Du, M.J. Yang, M.Y. Li, J. Yang, B. Peng, H. Li, et al., Metabolic mechanism for L-leucine-induced metabolome to eliminate *Streptococcus iniae*, J. Proteome Res. 16 (2017) 1880–1889.
[40] D. Saleiro, L.C. Platanias, Intersection of mTOR and STAT signaling in immunity, Trends Immunol. 36 (2015) 21–29.
[41] T. Schaumann, D. Kraus, J. Winter, M. Wolf, J. Deschner, A. Jager, Potential immune modularly role of glycine in oral gingival inflammation, Clin. Dev. Immunol. 2013 (2013) 808367.
[42] M. Ahmadian, J.M. Suh, N. Hah, C. Liddle, A.R. Atkins, M. Downes, R.M. Evans, PPARc signaling and metabolism: the good, the bad and the future, Nat. Med. 19 (2013) 557–566.
[43] L. Wang, B. Waltenberger, E.M. Pferschy-Wenzig, M. Blunder, X. Liu, C. Malainer, T. Blazevic, S. Schwaiger, J.M. Rollinger, E.H. Heiss, D. Schuster, B. Kopp, R. Bauer, H. Stuppner, V.M. Dirsch, A.G. Atanasov, Natural product agonists of peroxisome proliferator-activated receptor gamma (PPARc): a review, Biochem. Pharmacol. 92 (2014) 73–89.
[44] G.A. Robinson, K.E. Waddington, I. Pineda-Torra, E.C. Jury, Transcriptional regulation of T-cell lipid metabolism: implications for plasma membrane lipid rafts and T-cell function, Front. Immunol. 8 (2017) 1636.
[45] J.H. Chung, A.Y. Seo, S.W. Chung, M.K. Kim, C. Leeuwenburgh, B.P. Yu, H.Y. Chung, Molecular mechanism of PPAR in the regulation of age-related inflammation, Ageing Res. Rev. 7 (2008) 126–136.
[46] M.J. Choi, E.J. Lee, J.S. Park, S.N. Kim, E.M. Park, H.S. Kim, Anti-inflammatory mechanism of galangin in lipopolysaccharide-stimulated microglia: critical role of PPAR-γ signaling pathway, Biochem. Pharmacol. 144 (2017) 120–131.